Research in Astron. Astrophys. **2012** Vol. **12** No. **12**, 1655–1665
http://www.raa-journal.org *http://www.iop.org/journals/raa*

***R**esearch in*
***A**stronomy and*
***A**strophysics*

Avoided crossings between non-radial modes in low mass RGB stars *

Jun-Jun Guo[1,2,3], Yan Li[1,2] and Xiang-Jun Lai[1,2]

[1] National Astronomical Observatories / Yunnan Observatory, Chinese Academy of Sciences, Kunming 650011, China; *guojunjun@ynao.ac.cn; ly@ynao.ac.cn*
[2] Key Laboratory for the Structure and Evolution of Celestial Objects, Chinese Academy of Sciences, Kunming 650011, China
[3] Graduate University of Chinese Academy of Sciences, Beijing 100049, China

Received 2012 March 5; accepted 2012 June 12

Abstract Non-radial p modes and g modes appear simultaneously in red giant stars. Their frequencies have different variation rates, causing their frequencies to become close during stellar evolution so that avoided crossings appear. The separation between regions where acoustic waves and gravity waves propagate for l = 1, 2 and 3 is different, which results in the coupling efficiency also being different. We present the results of numerical computations of the models we study. We find that the two kinds of modes for l = 2 and 3 need to be closer in frequency in order for a complete exchange to occur, compared to the case for modes with l = 1. Their scaled oscillation frequencies also present better regularity with evolution than modes with l = 1. In order to study the effect of the avoided crossings in detail, we set the mode which has the smallest mode inertia to be the p mode. We plot the two kinds of modes for l = 1, 2 and 3 in frequency and period échelle diagrams and find modes of l = 2 and 3 fit the two relations better; they are more equally spaced in frequency and period than modes with l = 1. Under careful observation of the two kinds of échelle diagrams for l = 2 and 3, we still find that some p modes shift a little from being equally spaced in frequency and some g modes, which are close to those p modes in period, shift a little from being equally spaced in period. Then, we study the relation between the deviation from period being equally spaced and the mode inertia of g modes for different l. The g modes of l = 1 with a period closer to the p mode have less inertia and the deviation is bigger in the period échelle diagram. Their deviation is also obvious. However g modes of l = 2 and 3 shift a little or have almost no deviation from being equally spaced in period, even though some of them may have strong coupling and close mode inertia like in the p modes. So, we suggest a possible method for measuring period spacing of g modes precisely using mixed g modes with l = 2 and 3 that have fewer observed mixed g modes than for l = 1.

Key words: stars: oscillations — stars: red giants

* Supported by the National Natural Science Foundation of China.

1 INTRODUCTION

Low-mass red giants are characterized by an extended convective envelope and a contracting degenerate helium core. The turbulent motions in the convective envelope stochastically excite solar-like oscillations. Recently, the CoRoT and Kepler missions provided high-quality observational data for hundreds of red-giant stars (Bedding et al. 2010; Huber et al. 2010), including both p modes and mixed g modes. The observed mixed g modes in individual red giants provide new information on the stellar interior and have begun to be widely studied (Miglio et al. 2008a; Aerts et al. 2010; Bedding et al. 2011). Bedding et al. (2011) used the period spacing of mixed g modes with $l = 1$ to distinguish between hydrogen and helium burning stages of red giants. Mosser et al. (2012) showed that mixed g modes can be used to probe the thin hydrogen burning shell. Christensen-Dalsgaard (2011) indicated that measuring the period spacing may provide a method to determine the size of the convective core in helium-burning red giants. Beck et al. (2012) used the rotational frequency splitting of $l = 1$ mixed g modes to demonstrate that the core must rotate at least ten times faster than the surface.

Owing to contraction of the helium core, the buoyancy frequency can reach very large values in red giants and produce high frequency g modes. The frequencies of some g modes may coincide with those of p modes and undergo the avoided crossing (Aizenman et al. 1977; Dupret et al. 2009). Because of the occurrence of avoided crossings, p modes of $l = 1$ shift from being equally spaced in frequency, but radial modes ($l = 0$) follow the pattern of regular spacing with a separation of $\Delta\nu$ (Christensen-Dalsgaard 2004). The coupling efficiency between p and g modes becomes weaker for higher degrees of spherical harmonics (Dziembowski et al. 2001), and with the evolution of red giants, the interaction of $l = 1$ modes also becomes weaker because gravity waves are more easily trapped in the stellar interior and hence are well separated from the region where acoustic waves propagate (Montalbán et al. 2010; Huber et al. 2010). The properties of avoided crossing for $l = 1$ modes have been well studied, but $l = 2$ and 3 modes have not been considered extensively. In this paper we will focus on properties and effects of the avoided crossing for $l = 2$ and 3 modes, and provide a new method to determine period spacing using mixed g modes with $l = 2$ or 3.

The following sections are organized as follows: We briefly introduce stellar evolution models and general properties of adiabatic oscillations for our calculated red giant branch (RGB) models in Section 2. In Section 3, we investigate the effect of an avoided crossing between non-radial modes in detail, especially focusing on $l = 2$ and 3 modes. Discussions and conclusions are summarized in Section 4.

2 PROPERTIES OF STELLAR EVOLUTION MODELS AND ADIABATIC OSCILLATIONS

We use a stellar evolution code originally written by Paczynski and Kozlowski and updated by Sienkiewicz. The equation of state comes from the OPAL equation of state (Rogers 1994; Rogers et al. 1996). The OPAL opacities GN93hz series (Rogers & Iglesias 1995; Iglesias & Rogers 1996) are used in the high temperature case and Alexander's opacity tables (Alexander & Ferguson 1994) are used in the low temperature case. Element diffusion is only included in the main sequence. Convective heat transfer is treated by the standard mixing-length theory with the mixing-length parameter $\alpha = 1.70$. Convective overshooting and rotation are not included.

We calculate a series of stellar evolution models of $1.0 M_{\odot}$, with the initial chemical composition of hydrogen mass fraction $X = 0.7$ and metal mass fraction $Z = 0.02$. The evolution of the model is simulated from the pre-main sequence until the helium flash. We choose five stellar models spread along the RGB to calculate their typical parameters, with model 3 being at the middle stage while models 1 and 2 are in the early stage and models 4 and 5 are in the later stage of the RGB. Table 1 summarizes their basic properties.

Table 1 Typical Parameters of Calculated Models in Different Stages of Evolution

model	age(Gyr)	lg ($T_{\rm eff}$)(K)	R ($R_\odot$)	lg ($L/L_\odot$)	$\nu_{\rm max}$ (μHz)	$\Delta\nu$ (μHz)	$\Delta P_{\rm g}$ (s)
1	11.64242	3.67637	2.7883	0.549295	444.3	31.02	164.4–177.6
2	11.85505	3.66807	4.2031	0.872577	197.4	16.73	130.06–133.99
3	11.94962	3.65885	5.8832	1.127771	99.6	10.13	114.04–115.63
4	12.03602	3.64270	9.4738	1.476995	40.0	4.986	88.36–88.52
5	12.10987	3.59366	29.0302	2.253509	4.51	0.973	69.225–69.227

For high-order and low-degree p modes, they are regularly spaced in frequency, approximately following the asymptotic relation (Tassoul 1980)

$$\nu_{nl} \approx \left[2\int_0^R \frac{dr}{c}\right]^{-1}\left(n_{\rm p}+\frac{1}{2}l+\epsilon\right)=\Delta\nu\left(n_{\rm p}+\frac{1}{2}l+\epsilon\right), \tag{1}$$

where $n_{\rm p}$ is the radial order in the region where acoustic oscillations propagate. $\Delta\nu$ is the inverse of twice the sound travel time between the center and the surface. ϵ is a phase constant which is sensitive to the surface layers.

For g modes, they are regularly spaced in period, approximately following the asymptotic theory (Tassoul 1980; Miglio et al. 2008a)

$$P_{n_{\rm g},l} \approx \frac{2\pi^2(n_{\rm g}+\alpha_{\rm g})}{\sqrt{l(l+1)}}\left[\int_{r_1}^{r_2}\frac{N}{r}dr\right]^{-1}=\frac{\Delta P_{\rm g}(n_{\rm g}+\alpha_{\rm g})}{\sqrt{l(l+1)}}=\Delta P_l(n_{\rm g}+\alpha_{\rm g}) \tag{2}$$

where $n_{\rm g}$ is the radial order in the region where gravity oscillations propagate. $\alpha_{\rm g}$ is an unknown constant, ΔP_l is the period spacing for spherical harmonic degree l and $\Delta P_{\rm g}$ is related to ΔP_l and l.

The oscillation properties of non-radial modes are determined by the Brunt-Väisälä frequency and Lamb frequency (S_l). We present the propagation diagram of $l = 1$, 2, and 3 for model 3 in Figure 1. It can be seen that the Brunt-Väisälä frequency reaches a very large value in the helium core, which forms a region where gravity waves propagate. Acoustic waves propagate through the region in the stellar envelope, and there is a thin region where dissipation occurs between the two regions where propagation occurs.

From Figure 1, we can see that the region where gravity waves propagate with different frequencies has almost the same inner boundary r_1 but a different outer boundary r_2. The period spacing ΔP_l is determined by the integral in Equation (2), which is proportional to N and inversely proportional to r.

In Table 1, $\Delta P_{\rm g}$ is given for those g modes with a frequency range about 28 times as large as $\Delta\nu$. It can be seen that $\Delta P_{\rm g}$ changes less for g modes in stellar models during later stages of evolution on the RGB, which indicates that those g modes are approximately equally spaced in period in the middle and late stages of the RGB. $\nu_{\rm max}$ corresponds to the maximum of the acoustic power (Kjeldsen & Bedding 1995).

3 AVOIDED CROSSINGS BETWEEN NON-RADIAL P AND G MODES

Full equations of linear and adiabatic oscillations are numerically solved for model 3 to obtain eigenfrequencies and eigenfunctions of non-radial modes. In order to get accurate results, we use more than 30 000 grid points in the stellar evolution models.

3.1 Avoided Crossings during the Stellar Evolution

From Equations (1) and (3), we can see that the large frequency separation results from the time it takes for sound to travel between the center and the surface, while the period spacing is a conse-

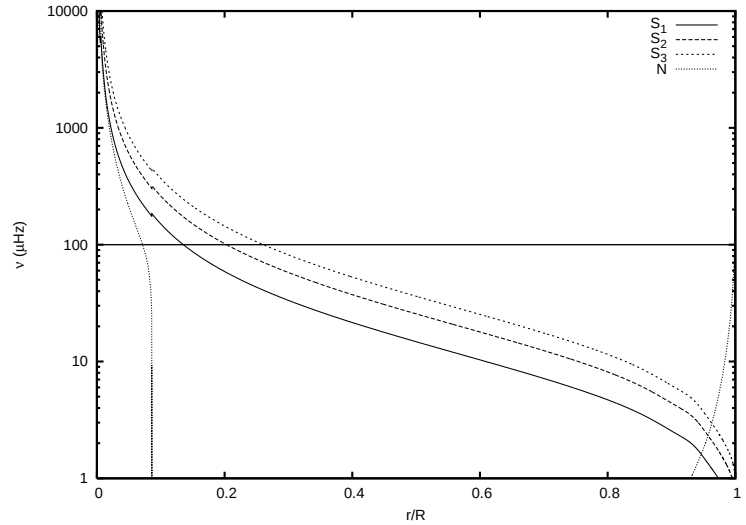

Fig. 1 The Brunt-Väisälä frequency (N) and Lamb frequency (S_l) are shown against fractional radius r/R for model 3. The horizontal line indicates a mode with frequency of $\nu = 100$ μHz.

quence of the distribution of Brunt-Väisälä frequency (N) in the region where gravity waves propagate, so the scaled rate of oscillation frequency for p modes is different from that for g modes. Kjeldsen & Bedding (1995) give the scaling relation of $\Delta\nu$ as

$$\Delta\nu \sim M^{1/2}/R^{3/2}. \tag{3}$$

Therefore, the scaled oscillation frequency $(R/R_\odot)^{3/2}\nu$ of the p modes should be almost unchanged with evolution, including the p modes of $l = 1$, 2, and 3, which change little when not being affected by the avoided crossing. However, for non-radial g modes of $l = 1$, 2, and 3, their scaled oscillation frequencies rise quickly with evolution when not being affected by the avoided crossing. Therefore, the scaled frequency of a g mode will increase until it is close to that of a p mode as the stellar evolution continues, promoting the coupling between acoustic waves in the envelope and gravity waves in the core. Finally, they exchange characteristics with each other, with p modes becoming g modes and g modes becoming p modes, and all of the original modes evolve along the evolutionary track of the other mode. It can be found, from the middle and lower panels in Figure 2, that avoided crossings exist in the non-radial p modes and g modes of $l = 2$ and 3, like the case for modes of $l = 1$, and their evolutionary tracks show better regularity. The larger the spherical harmonic degree l is, the closer the two kinds of modes need to be located on the evolutionary tracks to interact with each other.

3.2 Eigenfunctions of Non-Radial Modes

Examples of eigenfunctions with $l = 2$, which are the scaled radial displacement of a p-mode with an eigen-frequency of 121.71 μHz and that of a g-mode with an eigen-frequency of 126.64 μHz, are given in the upper panel of Figure 3. It can be seen that the p mode is well trapped in the stellar envelope and the g mode propagates dominantly in the helium core. The normalized mode inertia provides a rough estimate of the surface amplitude of an oscillation mode (Houdek et al. 1999). Generally speaking, the smaller inertia a mode has, the bigger the surface amplitude is. G modes usually have much larger scaled amplitudes than p modes in the core, as shown in the upper panel

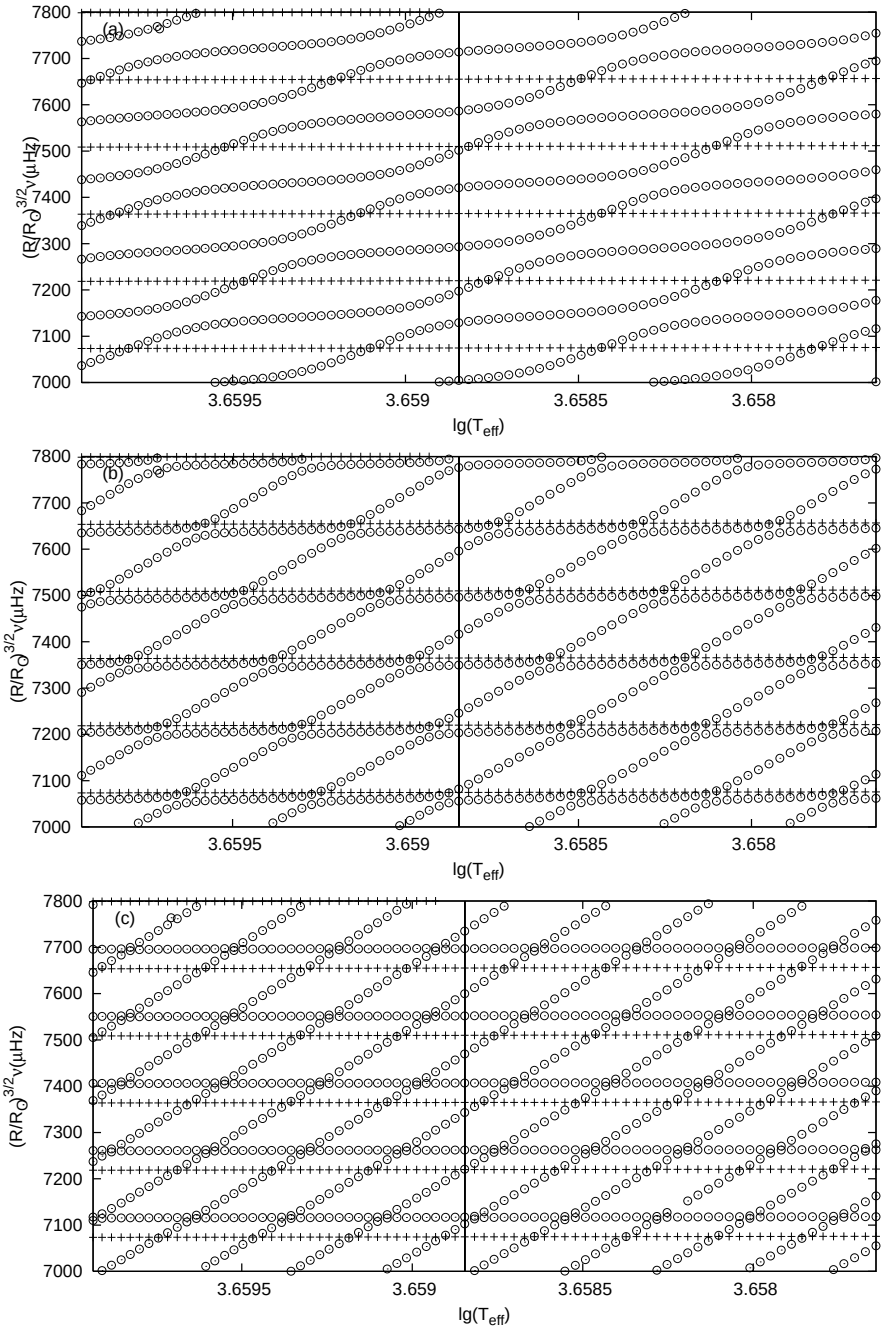

Fig. 2 Scaled oscillation frequencies, as functions of the effective temperature for modes of l = 0, 1, 2, and 3. The heavy vertical line in each diagram represents the results of model 3. The range of the models in radius and luminosity is 5.6762–6.1166 $R_{\odot}$ and 12.619–14.346 $L_{\odot}$, respectively. Modes of l = 0 are used for comparison. (a) Circles for l = 1 and pluses for l = 0. (b) Circles for l = 2 and pluses for $l = 0$. (c) Circles for l = 3 and pluses for l = 0.

of Figure 3. As a result, g modes have much larger mode inertias than p modes and are less likely to be observed.

However, some g modes with frequencies sufficiently close to p modes will undergo avoided crossings and their acoustic waves couple with gravity waves to form mixed modes. It can be seen in the lower panel of Figure 3 that a mixed g mode with an eigen-frequency of 121.57 μHz has a scaled amplitude in the two regions where propagation occurs that is close to the p-mode mentioned in the upper panel. Such a mixed g mode acts like a p mode that needs a small inertia and a large surface amplitude to be observable (Beck et al. 2011; Bedding et al. 2011). In this sense, the mixed g mode has been interacting with the p mode and the region where its acoustic wave propagates has been coupling with the region where the gravity wave propagates. In this paper, we set the modes with the smallest inertia as p modes and others are identified as g modes.

3.3 Deviations from Two Equal Spacing Relations for p and g Modes

For a given stellar model such as model 3, we can investigate the effects of avoided crossings on periods or frequencies of non-radial modes. We focus on modes in a frequency range (210 μHz – 560 μHz). In such a high frequency range, the coupling efficiency between acoustic waves in the envelope and gravity waves in the core is higher since the separation between the two regions where propagation occurs is smaller, as shown in Figure 1, which indicates that those two regions can be more easily coupled. On the other hand, due to relatively larger separation of their spacings, there are fewer g modes between the two adjacent p modes.

In order to clearly show the effects of avoided crossings on frequencies of non-radial modes, we define a reduced frequency $\hat{\nu}$ as

$$\nu_{nl} = \nu_0 + k\Delta\nu + \hat{\nu}_{nl} \tag{4}$$

and a reduced period $\hat{P}$ as

$$P_{n_g,l} = P_0 + k\Delta P_l + \hat{P}_{nl}, \tag{5}$$

where ν_0 and P_0 are zero, $\Delta\nu$ and ΔP_l are constants, and k is taken as an integer that makes $\hat{\nu}_{nl}$ be between 0 and $\Delta\nu$ and $\hat{P}_{nl}$ be between 0 and ΔP_l. In Figure 4 we show the results of model 3. The left panels are the échelle diagrams of frequency with $\hat{\nu}_{nl}$ as the abscissa and ν_{nl} as the ordinate, while the right panels corresponding to the left panels are the échelle diagrams of period with $\hat{P}_{nl}$ as the abscissa and P_{nl} as the ordinate. It can be seen in the échelle diagrams of frequency that p modes of $l = 2$ and 3 are almost equally spaced in frequency and g modes of $l = 2$ and 3 scatter stochastically. In the échelle diagrams of period, however, g modes of $l = 2$ and 3 are almost equally spaced in period and p modes of $l = 2$ and 3 scatter irregularly. By comparing these two kinds of échelle diagrams we can easily recognize p modes and g modes. Under careful observations of these panels, we find that some p modes of $l = 2$ shift slightly from the relation of equal spacing in frequency and some g modes of $l = 2$ shift slightly from the relation of equal spacing in period. In addition, at almost the same frequency or period in the two kinds of échelle diagrams, we can always find a mode with a different characteristic accompanying those modes which shifts slightly from the equal spacing relations. This phenomenon is a clear demonstration of avoided crossings between the two interacting modes. Modes of $l = 3$ show a similar phenomenon, but the deviation is much less obvious or even difficult to see. However, most modes of $l = 1$ obviously shift from these equal spacing relations, indicating that avoided crossings are much more common in $l = 1$ non-radial p and g modes.

3.4 Relation of Period Deviation and Mode Inertia for g Modes with Different l

In the low frequency range, there are many g modes located between two adjacent p modes, since the relative frequency spacing of g modes decreases when the frequency decreases. This results in

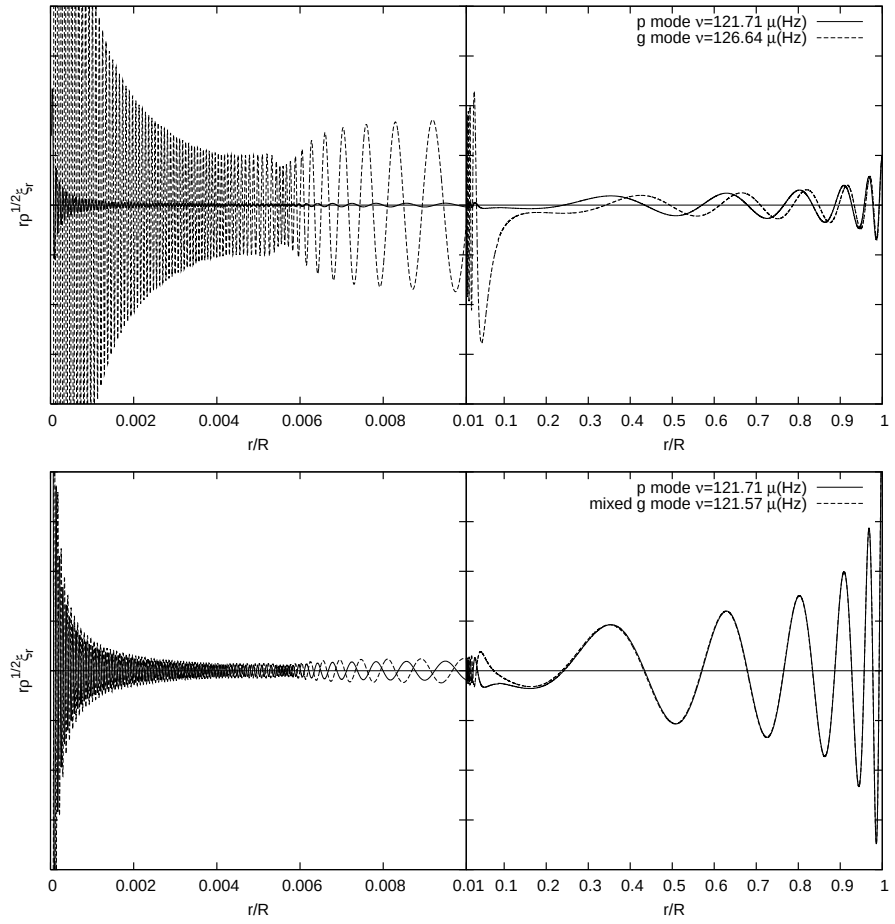

Fig. 3 The upper panel shows scaled radial displacement eigenfunctions for a p mode (*continuous line*) with l = 2, $n_{\rm p}$ = 11, and ν = 121.71 μHz and a g mode (*dashed line*) with l = 2, $n_{\rm g}$ = –168, and ν = 126.64 μHz. The lower panel shows scaled radial displacement eigenfunctions for the same p mode as the upper panel (*continuous line*) and a g mode (*dashed line*) with l = 2, $n_{\rm g}$ = –175, and ν = 121.75 μHz. The left two panels show the scaled eigenfunctions in the inner one percent of the radius of the model we chose. The surface amplitude has been normalized in this figure. For clarity, the curve for the scaled eigenfunctions has been truncated.

more g modes interacting with a p mode because their frequencies are sufficiently close to each other. But this trend is different for modes of l = 1, 2, and 3 due to different coupling efficiency. In Figure 5 we show the effect of avoided crossings on the degree of period deviation and the mode inertia of g modes with $l = 1$ in a frequency range of (70 μHz – 140 μHz). We can see several g modes obviously shift from being equally spaced in period around every p mode in the left panel, and a g mode deviating more from the equal spacing relation will have less mode inertia through comparing with the right panel. In addition, a g mode will deviate in the échelle diagram of period to the right when its period is greater and to the left when its period is less than that of the p mode it surrounds. For $l = 2$ modes in Figure 6, there are less g modes shifted from being equally spaced in period around every p mode. Their degree of period deviation is also less than the case for $l = 1$

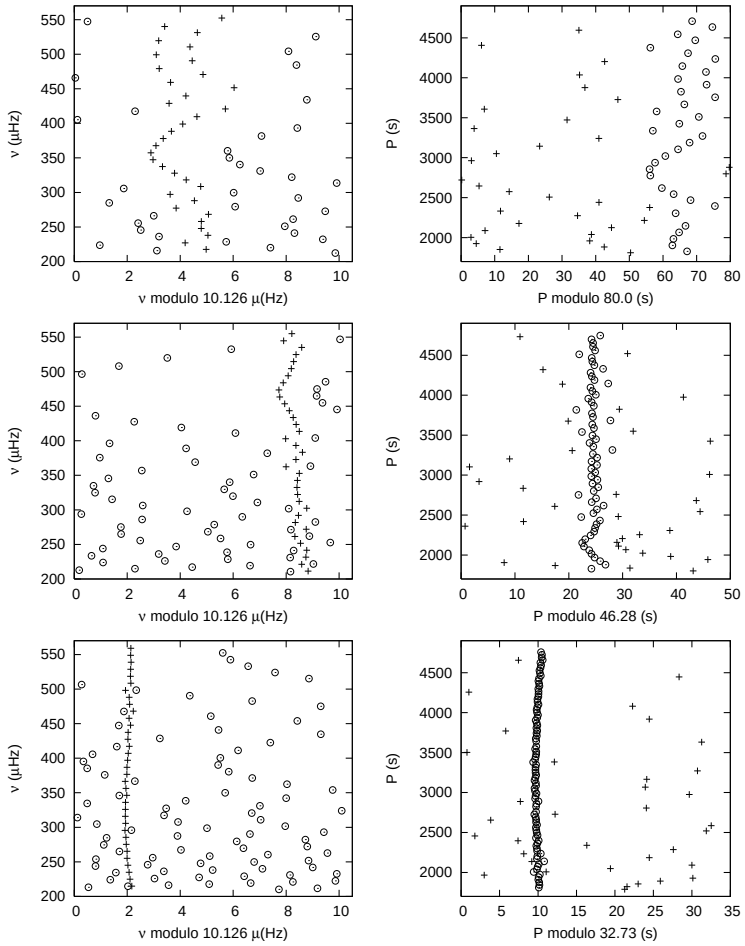

Fig. 4 The left three panels are frequency échelle diagrams for l = 1, 2, and 3 respectively with modulo $\Delta\nu$ = 10.126 (μHz). The right three panels are period échelle diagrams with modulo ΔP_1 = 80.00 (s), ΔP_2 = 46.28 (s), and ΔP_3 = 32.73 (s), all of which correspond to the figure in the left panel. In each panel, there are pluses for p modes and circles for g modes.

even though some g modes of $l = 2$ have almost the same inertia as the p mode has. As seen in Figure 7, g modes with $l = 3$ show almost no deviations from the equal spacing relation in period, although some of them may have inertia close to that of the p mode. Therefore, some g modes with $l = 2$ and 3 are able to be observed, and the fact that they show little deviation from being equally spaced in period makes them a better candidate for precise determination of period spacing.

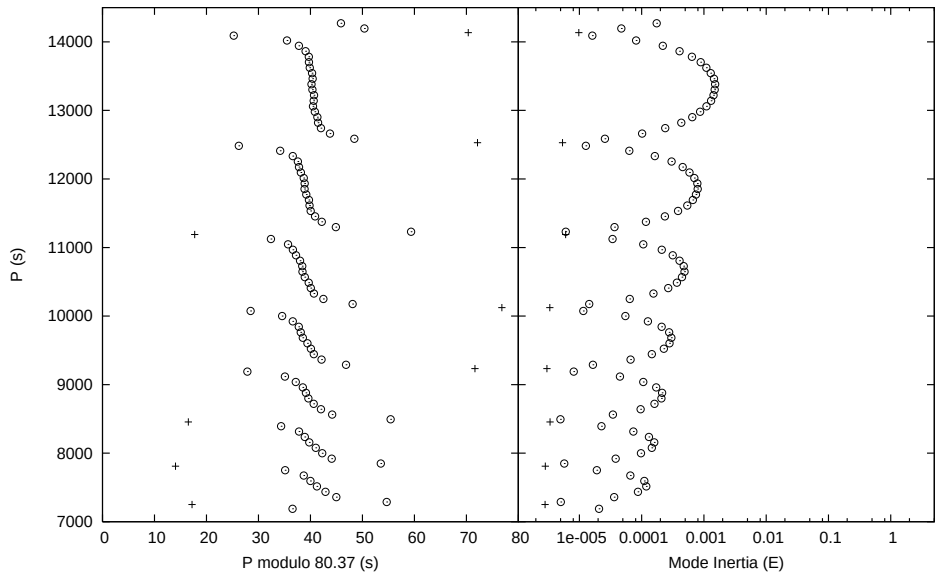

Fig. 5 The left panel is the period échelle diagram for l = 1 modes with modulo ΔP_1 = 80.37 (s). The right panel shows the mode inertia for the abscissa corresponding to the left panel. There are pluses for p modes and circles for g modes in every panel.

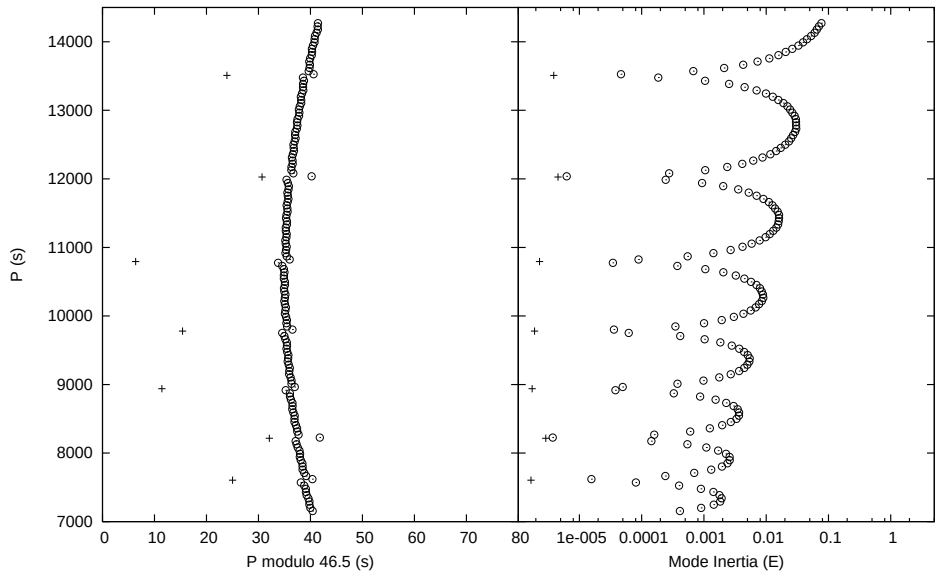

Fig. 6 The left panel is the period échelle diagram for l = 2 modes with modulo ΔP_2 = 46.5 (s). The right panel shows the mode inertia for the abscissa corresponding to the left panel. There are pluses for p modes and circles for g modes in every panel.

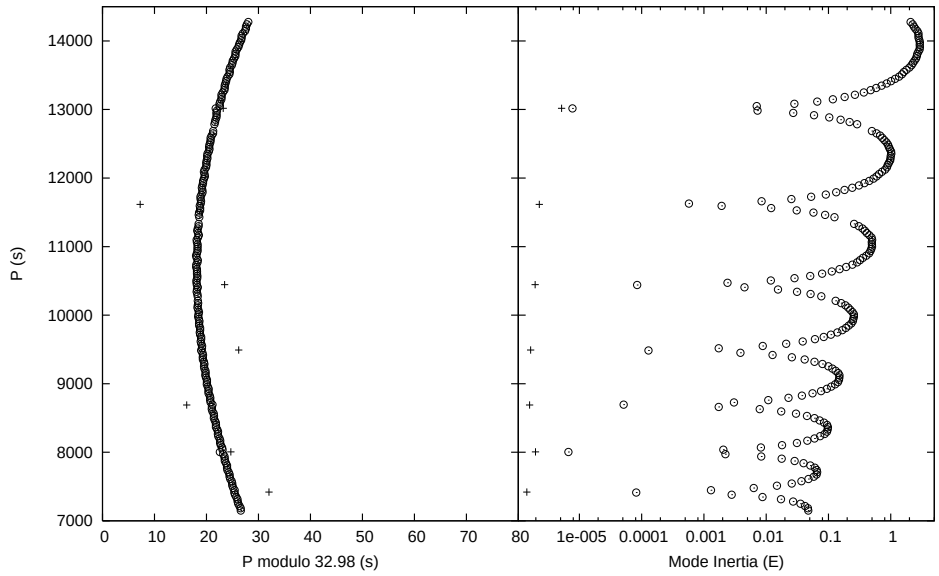

Fig. 7 The left panel is the period échelle diagram for l = 3 modes with modulo ΔP_3 = 32.98 (s). The right panel shows the mode inertia for the abscissa corresponding to the left panel. There are pluses for p modes and circles for g modes in every panel.

4 CONCLUSIONS AND DISCUSSION

In this paper, we present the results of a detailed investigation on avoided crossings for non-radial modes of l = 1, 2 and 3 in low-mass RGB stars. We have found that p and g modes of l = 2 and 3 need to be closer in frequency to interact with each other than modes of l = 1. Their scaled oscillation frequencies also show better regularity with evolution than modes of l = 1. In the place of an avoided crossing, we find that some p modes shift from being equally spaced in frequency and some g modes which are close to those p modes shift from being equally spaced in period. Modes of l = 1 obviously shift from the two relations, but modes of l = 2 and 3 shift less or have almost no deviation from them. In addition, g modes of l = 1 with a period closer to p modes have less inertia and the deviation is bigger in the period échelle diagram. However, g modes of l = 2 and 3 shift slightly or have almost no deviation from being equally spaced in period even though some of them may have strong coupling and a close mode inertia like the p mode has.

At present, many mixed g modes of l = 1 have been observed. They are widely used in detecting the internal structure and evolution of RGB stars, but mixed g modes of l = 2 and 3 are not well studied since few of them have been observed. With new methods of observation and progress in technology, more mixed g modes of l = 2 and 3 will be observed in the future. Because they better fit the relation of being equally spaced in period, we can use them to precisely measure period spacing, even with fewer mixed g modes of l = 2 and 3.

Acknowledgements This work is supported by the National Natural Science Foundation of China (Grant Nos. 10973035 and 10673030), the Knowledge Innovation Key Program of the Chinese Academy of Sciences under Grant No. KJCX2-YW-T24 and the Yunnan Natural Science Foundation (Y1YJ011001). Fruitful discussions with Q.-S. Zhang, C.-Y Ding, J. Su, T. Wu and Y.-H. Chen are highly appreciated.

References

Aerts, C., Christensen-Dalsgaard, J., & Kurtz, D. W. 2010, Asteroseismology, Astronomy and Astrophysics Library, Volume. ISBN 978-1-4020-5178-4 (Springer Science+Business Media B.V.)
Aizenman, M., Smeyers, P., & Weigert, A. 1977, A&A, 58, 41
Alexander, D. R., & Ferguson, J. W. 1994, ApJ, 437, 879
Beck, P. G., Bedding, T. R., Mosser, B., et al. 2011, Science, 332, 205
Beck, P. G., Montalban, J., Kallinger, T., et al. 2012, Nature, 481, 55
Bedding, T. R., Huber, D., Stello, D., et al. 2010, ApJ, 713, L176
Bedding, T. R., Mosser, B., Huber, D., et al. 2011, Nature, 471, 608
Christensen-Dalsgaard, J. 2004, Sol. Phys., 220, 137
Christensen-Dalsgaard, J. 2011, arXiv:1106.5946
Dupret, M.-A., Belkacem, K., Samadi, R., et al. 2009, A&A, 506, 57
Dziembowski, W. A., Gough, D. O., Houdek, G., & Sienkiewicz, R. 2001, MNRAS, 328, 601
Houdek, G., Balmforth, N. J., Christensen-Dalsgaard, J., & Gough, D. O. 1999, A&A, 351, 582
Huber, D., Bedding, T. R., Stello, D., et al. 2010, ApJ, 723, 1607
Iglesias, C. A., & Rogers, F. J. 1996, ApJ, 464, 943
Kjeldsen, H., & Bedding, T. R. 1995, A&A, 293, 87
Miglio, A., Montalbán, J., Eggenberger, P., & Noels, A. 2008a, Astronomische Nachrichten, 329, 529
Miglio, A., Montalbán, J., Noels, A., & Eggenberger, P. 2008b, MNRAS, 386, 1487
Montalbán, J., Miglio, A., Noels, A., Scuflaire, R., & Ventura, P. 2010, ApJ, 721, L182
Mosser, B., Elsworth, Y., Hekker, S., et al. 2012, A&A, 537, A30
Rogers, F. J. 1994, in IAU Colloq. 147: The Equation of State in Astrophysics, eds. G. Chabrier & E. Schatzman (Cambridge: Cambridge Univ. Press), 16
Rogers, F. J., & Iglesias, C. A. 1995, in Astronomical Society of the Pacific Conference Series, 78, Astrophysical Applications of Powerful New Databases, eds. S. J. Adelman, & W. L. Wiese (San Francisco: ASP), 31
Rogers, F. J., Swenson, F. J., & Iglesias, C. A. 1996, ApJ, 456, 902
Tassoul, M. 1980, ApJS, 43, 469